NASA Technical Memorandum 87727

NASA-TM-87727 19860017737

EVALUATION OF THREE NUMERICAL METHODS FOR PROPULSION INTEGRATION STUDIES ON TRANSONIC TRANSPORT CONFIGURATIONS

STEVEN F. YAROS, JOHN R. CARLSON,
AND BALASUBRAMANYAN CHANDRASEKARAN

JUNE 1986

National Aeronautics and
Space Administration

Langley Research Center
Hampton, Virginia 23665

SUMMARY

An effort has been undertaken at the NASA Langley Research Center to assess the capabilities of available computational methods for use in propulsion integration design studies of transonic transport aircraft, particularly of pylon/nacelle combinations which exhibit essentially no interference drag. The three computer codes selected represent state-of-the-art computational methods for analyzing complex configurations at subsonic and transonic flight conditions. These are: EULER, a finite volume solution of the Euler equations; VSAERO, a panel solution of the Laplace equation; and PPW, a finite difference solution of the small disturbance transonic equation. In general, all three codes have certain capabilities that allow them to be of some value in predicting the flows about transport configurations, but all have limitations. Until more accurate methods are available, careful application and interpretation of the results of these codes are needed.

INTRODUCTION

Future transport aircraft must offer improved performance at lower cost if the competitive position of the airlines is to be preserved (see ref. 1). Many advanced technologies will be required for this task. With respect to the airframe/propulsion integration area, it will be necessary to minimize the drag associated with the powerplant installations and then attempt to achieve favorable interference effects, if possible. This work will require an extensive integration program including both experimental studies and theoretical methods, with the latter being used to predict the results of configuration changes as well as to guide the experimental programs.

Recently an effort has been undertaken at the NASA Langley Research Center to assess the capabilities of available computational methods for use in propulsion integration design studies of transonic transport configurations. The configurations of interest consisted of a body, wing, wing-mounted pylon, and a pylon-mounted nacelle. Configurations which included more than one pylon and nacelle per wing, any sort of wing-top-mounted engines, and any fuselage-mounted engines were specifically excluded. The objective of these studies is to design pylon/nacelle combinations which exhibit essentially no interference drag. As a first step toward this goal, an assessment of the capabilites of three computer codes, all of which were designed for complex aircraft configurations, was made. The configuration selected for the code validation was a low-wing transport configuration, the Energy Efficient Transport (EET), which had been tested previously in the 8-Foot Transonic Wind Tunnel at the NASA Langley Research Center (reference 2). A computer-generated picture of the EET is shown in figure 1. The validity of further flow predictions for different transport configurations would be indicated by the performance of the codes on this baseline configuration.

The three computer codes selected for study represent state-of-the-art computational methods for analyzing complex configurations at subsonic and transonic flight conditions. Each of these codes will be described in some detail and the

validity of the predictions will be assessed via comparison with experimental data. Finally, the capabilities of these codes for use in propulsion integration design will be discussed.

SYMBOLS

b	wing span
C	wing chord
C_N	normal force coefficient
C_p	pressure coefficient
E	total energy, normalized to p_∞/ρ_∞
H	total enthalpy, normalized to p_∞/ρ_∞
M	Mach number
$\vec{n}$	unit normal vector
p	pressure, normalized to p_∞
$\vec{q}$	total velocity vector
t	time
V	total velocity $\sqrt{u^2 + v^2 + w^2}$
u,v,w	velocities in the x,y,z directions
x,y,z	longitudinal, lateral, and vertical cartesian coordinates
α	angle of attack
γ	specific heat ratio
ρ	density, normalized to ρ_∞

Subscripts:

ref	reference
x,y,z	partial derivatives
∞	free-stream conditions

PREDICTION METHODS

The three computer codes chosen for evaluation represent a spectrum of solution approaches. The first code, EULER, utilizes a finite-volume solution of the Euler equations; the second, VSAERO, is a panel method solution of the Laplace equation; and the third code, PPW, is based on a finite-difference solution of the small disturbance transonic equation. The following description of the three codes will emphasize their unique features.

Euler.- The Euler code used in this study is based on the work of Jameson, et. al. (ref. 3) and was modified by Yu, et. al. (ref. 4) to analyze the flow field of a wing-mounted propfan configuration. Thus the code has the capability of treating a wing/body configuration with or without a nacelle blended into the wing. As such, the code is used in the wing/body alone mode for this study. This particular modified version of the Euler code, however, may be useful for other turbofan configurations where the nacelles are mounted onto the wing, such as the Boeing 737.

In this method, the wing and fuselage are represented by a surface-fitted grid system (fig. 2). The finite volume grid consists of C-meshes around the wing section. The grid generation technologies used in this method include both elliptic finite difference and algebraic methods. For simple wing alone geometries, the flow program calculates the grid using the algebraic transformations from reference 5. For wing/body and wing/body/nacelle configurations, the grids are obtained using the elliptical grid generation solver (ref. 4). In this paper, the grids for the wing/body calculations have been obtained using the elliptic grid solver.

The Euler equations used for this code are written in the following form:

$$W_t + f_x + g_y + h_z = 0$$

where

$$W = \begin{bmatrix} \rho \\ \rho u \\ \rho v \\ \rho w \\ \rho E \end{bmatrix} \qquad f = \begin{bmatrix} \rho u \\ p + \rho u^2 \\ \rho uv \\ \rho uw \\ puH \end{bmatrix}$$

$$g = \begin{bmatrix} \rho v \\ \rho uv \\ p + \rho v^2 \\ \rho vw \\ \rho vH \end{bmatrix} \qquad h = \begin{bmatrix} \rho w \\ \rho uw \\ \rho vw \\ p + \rho w^2 \\ \rho wH \end{bmatrix}$$

The boundary condition along the surface is given by

$$\vec{q} \cdot \vec{n} = 0$$

This relationship together with a normal momentum relationship are used to define the surface pressure. Along the far field boundary, characteristic boundary conditions utilizing Riemann invariants are employed to impose free-stream conditions and to extract any unknown physical variables for the Euler solver. The equations together with the boundary condition are integrated in time using a fourth order Runge-Kutta time-stepping scheme. Because only the steady state solutions are of interest in the present study, a local time step is used at every mesh cell in the time integration procedure to speed up convergence.

The method includes a two-dimensional strip theory boundary layer on the wing coupled with the outer flow. The boundary layer is calculated by Green's lag-entrainment method (ref. 6). The calculated boundary layer effect is suitably incorporated in a transpiration source term, and this replaces the surface boundary condition on the wing. This approach eliminates the need to regenerate the grids for each revised configuration as would be done in a displacement thickness model.

VSAERO.- VSAERO (Vortex Separation Aerodynamic Program) is a surface singularity solution to the Laplace equation using quadrilateral panels to represent arbitrary three-dimensional bodies. Source and doublet singularities are distributed in a piecewise constant fashion on each panel. Neumann boundary conditions are applied to the panel to determine the singularity strength. Dirichlet boundary conditions are applied at the boundary to determine the doublet strength. More detailed discussions of this method appear in references 7 and 8.

The code includes features such as wake shape iteration, jet wakes, on- and off-body streamline calculations, and off-body velocity calculations. Jet wakes, in particular, are modeled using doublet sheets with a linear variation in doublet strength in the streamwise direction. For our cases a flat wake was assumed at first, with one iteration redefining its shape. Flow-through nacelles can be modeled by specifying a unit normal velocity on the inlet face and a corresponding outflow at the exhaust. The major limitation in the use of the code, of course, is the incompressible nature of the basic equation. Transonic results may be approximated through the use of the Karman-Tsien compressibility correction. The VSAERO code is capable of modeling the full geometry of the EET configuration: body, wing, pylon, and nacelle.

The geometric description of the aircraft configuration is based on panels, patches, and wakes, which can be combined to form components and assemblies. Some automatic capabilities are provided in the code for paneling and also patch generation in special situations. The computer generated picture of the EET in figure 1 was produced from data to be input to the VSAERO code.

The effects of viscosity are calculated using a two-dimensional, integral boundary layer calculation (ref. 9). The calculations follow surface streamlines that have been determined from an initial potential flow calculation. The boundary layer thickness from this calculation is simulated by surface transpiration, and a new potential calculation is performed using the transpiration velocities.

PPW.- The PPW (Pod-Pylon-Winglet) code is actually WIBCO-PPW, which indicates its heritage as an expanded version of an older code, WIBCO (ref. 10). The code was developed specifically for arbitrary wing-body configurations with any combination of pods (nacelles), pylons, and winglets. PPW is thus able to model the full EET configuration.

The distinguishing feature of the PPW code is its use of multiple embedded grid systems, as shown in figure 3. The global grid, also known as the crude grid, is stretched to infinity in all directions, and thus includes the entire aircraft configuration. Auxiliary grid systems, of finer grid spacing and limited ranges, are able to be placed in areas where there is particular interest. As in the original WIBCO code, both the body and the wing have their own fine grid system, but the PPW code has additional fine grid systems for the nacelles, pylons, and winglets. All of the grid systems are Cartesian. This involves certain approximations in the definition of the surfaces in the embedded fine grid systems. For the case of the pylon, for example, the physical pylon surface is approximated as a rectangular slab with leading and trailing edges coinciding with those of the wing at that span location. Other approximations involving the other components involve location of the component, point of application of the boundary conditions, and body shape corrections to the boundary conditions. In general, all such approximations are assumed to be small in comparison with the scale of the aircraft.

The equation used in the PPW code is the transonic small-disturbance flow equation with some additional terms retained from the full potential equation:

$$\left[1-M_\infty^2 - (\gamma+1)\, M_\infty^2\, \phi_x - \frac{\gamma+1}{2} M_\infty^2\, \phi_x^2 \right] \phi_{xx} - 2M_\infty^2\, \phi_y\, \phi_{xy}$$
$$+ \left[1 - (\gamma-1)M_\infty^2\, \phi_x \right] \phi_{yy} + \phi_{zz} = 0$$

where ϕ is the disturbance velocity potential. The retained terms, which are the non-linear terms, are used to resolve shock waves for highly swept wings. Solution of the equation is done by successive line over-relaxation, where the vertical columns of grid points are relaxed starting at the first point upstream.

The solutions of the individual fine embedded grid systems are passed to the global grid system and to each other, the exact procedure depending on the configuration components. Central differencing is used throughout, except for second derivatives in local supersonic conditions, where upwind differencing is used.

Viscous effects may be added to the wing, and the PPW code has the capability of calculating flow solutions from any level of viscous/inviscid iterations. The basic 2-D boundary layer method used is that of Bradshaw and Ferriss (ref. 11). To aid in simulating three-dimensional effects, the modifications of Nash and Tseng (ref. 12) for flow about an infinite yawed wing, are applied. The boundary layer displacement thickness, or a portion of it in near-separated regions, is added to the basic wing shape at each new inviscid iteration. Boundary-layer shape is then updated with the new pressure distribution. Additional details concerning transition location, boundary layer manipulation in regions of separation, and the effect of the boundary layer on the boundary conditions may be found in reference 10.

EXPERIMENTAL DATA

The experimental data, presented in reference 2, were obtained in the 8-Foot Transonic Wind Tunnel at NASA Langley Research Center. The EET configuration is

shown in figure 1. The aircraft is a low-wing advanced transport with a pylon-mounted nacelle located nominally at the 40% wing span position, where the wing thickness ratio is 12%. The wing itself is swept 30^{o} at the quarter-chord and has an aspect ratio of 9.8.

CODE VALIDATION

Numerous calculations were made with the three codes, and comparisons with the data available were used where possible. The results were compared primarily with the wing pressure coefficient distribution at several spanwise locations. Results are shown herein only at a 2y/b of 0.4280, which corresponds to a position just outboard of the pylon location. Results at other locations display characteristics and trends similar to these results. Comparisons are made at model test conditions of $M_{\infty} = 0.70$, and $\alpha = 1.0^{o}$ and $M_{\infty} = 0.82$ and $\alpha = 2.8^{o}$, except for some comparison runs at varying Mach numbers. Span load distributions are also presented in some cases to emphasize the three-dimensionality of the wing pressure distribution and to indicate the capability of each code to predict wing loadings.

In this code evaluation, a study of the effect of grid sensitivity was not made. Changes in grid sizes and shapes can often affect lift, drag, and C_p distribution.

Pressure coefficients.- Chordwise pressure distributions are presented in figure 4 for both combinations of M_{∞} and α, with and without the pylon/nacelle. Figure 4 shows data that would be studied in any preliminary design work, and wind tunnel data are included for comparison purposes. Discrepancies between the two will indicate areas for further investigation. All of the theoretical curves have gone through a number of viscous/inviscid iterations and can be considered as "converged viscous solutions."

All three codes are able to provide predictions for the two wing-body (WB) cases, figures 4(a) and 4(c), whereas only the VSAERO and PPW methods can predict the flows for the wing-body-pylon-nacelle (WBPN) configuration, figures 4(b) and 4(d). Some general observations may be made.

At $M_{\infty} = 0.70$ and $\alpha = 1^{o}$, the wing/body predictions of all three codes, figure 4(a), are in reasonable agreement with experiment, although all of the methods show an overprediction of the C_p on the lower aft surface of the wing (the "cusp" region of the wing). This discrepancy may indicate an inadequate prediction of the boundary layer growth for all three methods.

The same general comments apply when the pylon and nacelle are added (fig. 4(b)). Both the PPW and VSAERO codes predict the pressure coefficient distribution in an accurate manner, with the exception of the pressure coefficient distribution on the aft lower surface of the wing.

If the predictions for the higher Mach number are examined, it appears that the Euler solution is fairly good for the WB case (fig. 4(c)). Comparing both WB cases, the Karman-Tsien compressibility correction in the VSAERO code results in a pressure coefficient distribution at the higher Mach number that is similar in shape to the distribution at the lower Mach number (fig. 4(a)). This characteristic holds true

when the pylon and nacelle are added, as can be seen in figure 4(d). The prediction is a scaled version of the solution at the lower Mach number, with no indication of shock wave formation.

By far the most striking change in flow prediction occurs for the PPW code at the higher Mach number (figs. 4(c) and 4(d)). In the prediction the shock is moved forward compared to the data by 10-15%. This discrepancy will be discussed later in this paper.

Span load distributions.- The span load distributions corresponding to these four cases are shown in figure 5. Noteworthy is that the PPW code predicts the span loading with respectable accuracy in all cases, in spite of the fact that the location of the predicted shock wave was grossly in error at the higher Mach number, as was seen in figures 4(c) and 4(d). The other methods do reasonably well for the WB case at the lower Mach number, especially the VSAERO code. The Euler code overpredicts the loading, possibly as a result of an insufficiently thick boundary layer, which will be discussed later. In both of the WBPN cases predicted by the VSAERO code, there is a slight discontinuity of loading across the pylon. This discontinutiy has been found to be sensitive to the geometric description of the wing and pylon intersection.

Code sensitivities.- It was noted that the predictions shown in figures 4 and 5 were viscous predictions, that is to say, the three methods went through sufficient viscous/inviscid iterations to stabilize on a solution that was consistent with the revised viscous boundary conditions, either transpiration or displacement thickness. An indication of viscosity effects on the converged solution is shown in figure 6(a), where the PPW viscous and inviscid solutions are compared to the data for the WB configuration at the higher Mach number. The qualitative effects, especially on the lower aft surface are expected. The fact that the inviscid solution also places the shock too far forward indicates that this discrepancy is not fully due to errors in the viscous interaction model.

Examination of the same solutions with the Euler code, figure 6(b), shows the insignificance of the predicted boundary layer in causing a change in the pressure distribution. This problem may be the cause of the span loading errors shown in figures 5(a) and 5(c), and indicates inadequate boundary layer modeling in the code.

The discrepancies in the predicted location of the upper surface shock wave in the case of the PPW code can be related to small changes in the specification of the free stream Mach number. In figures 7(a) and 7(b), which are inviscid predictions for the PPW and Euler codes, respectively, it is seen that as the free stream Mach number is changed from 0.78 to 0.86, the shock wave on the upper surface of the wing moves aft at least 60% X/c with both codes. At these Mach numbers, the introduction of viscosity would tend to move any shock wave 10% to 15% forward. The inviscid solution for the PPW code (figure 7(a)) is not satisfactory at a Mach number of 0.82, as there is still a strong indication of a double shock wave. Increasing the Mach number to 0.84 would greatly help the prediction for the PPW code, and this can be seen in figure 8, where both the viscous and inviscid solutions at 0.84 are compared to the data at $M_\infty = 0.82$.

This phenomenon was noted by Waggoner, both with the present PPW code (ref. 13) and its predecessor, WIBCO (ref. 14). Waggoner runs the code at a Mach number slightly elevated from the free-stream Mach number to take into account the "fuselage effect," which is not modeled into the code when only the crude grid is

used. The value of Waggoner's Mach number shift for the EET configuration at $M_\infty = 0.82$ is +0.007. This value was determined by analyzing an axisymmetric body with the EET area distribution and averaging the Mach number increment over the wing. Such an adjustment would improve the results presented herein, but the theoretical justification is based on empirical results.

Design sensitivities.- The rest of the results will focus on the sensitivity of the VSAERO and PPW codes to changes in pylon and nacelle configuration. Figures 9(a) and 9(b) show the results of pylon-nacelle buildup at the lower Mach number, 0.70. It can be seen immediately that the VSAERO results provide a continuous change in C_p distribution as the components are added, whereas the PPW code seems to divide its results into two "families": one with the nacelle and one without the nacelle. This result arises from the fact that the PPW representation of the pylon, as noted before, is a rough approximation of a real pylon. The division into two families is shown more clearly in figure 9(c) at the higher Mach number. These results indicate that the PPW code cannot be used in its present state for detailed pylon design studies.

If studies of nacelle design parameters are required from the PPW code however, the results can be considered useful in spite of the lack of data used for comparison, as can be seen in figures 10 and 11. Nacelle incidence change exhibits the expected change in C_p distribution, although it is rather small. The span loading, figure 11, also changes with a 10% 2y/b shift inboard, although the change is small. The span loadings shown in figure 11 were generated from inviscid runs, and are thus too high. The effect of viscosity in both cases would be merely to lower the curves, thus bringing them into better agreement with the data.

CONCLUDING REMARKS

Three computer codes have been investigated to determine their capabilities in predicting the flows about transport configurations. In general, none of the three codes are fully capable of predicting the flow about such a configuration, including pylons and nacelles, in transonic flow in sufficient detail or with sufficient accuracy to satisfy the stated requirements, i.e., to design pylons and nacelles with essentially no interference drag. However, each of the codes have some general capabilities which can be useful in predicting the flows about transport configurations.

The Euler code is capable of transonic flow predictions, and it has demonstrated satisfactory inviscid and fair viscous solutions for the wing-body configuration. The limited geometry capability of this Euler code precludes any form of turbofan on a pylon analysis, perhaps the most common configuration, because of the geometry requirement that the nacelle be blended into the wing. Therefore, it could not be compared to the other codes for the more complex geometries.

The VSAERO code provides for a good representation of the geometry of typical transport aircraft, but is hampered by the basic incompressible nature of its flow equation. The Karman-Tsen compressibility correction improves the predictions at higher Mach numbers, but it does not introduce the basic transonic non-linearities needed to model shock waves. In addition, the code has exhibited some calculation discrepancies in span loading near the pylon-nacelle areas.

The PPW code seems to have generated the best predictions overall, being the only code that covered the full range of configuration and test variables of the experimental data. The necessity of an empirical adjustment to the free-stream Mach number in order to properly predict shock locations needs further study. The current treatment of the pylon as a rectangular slab in the PPW code is also unsatisfactory, as it does not allow the full details of pylon design to be considered.

Although none of the three codes investigated completely meets the propulsion integration design study requirements, each of the codes may, given knowledge of the above restrictions, be useful as a limited design tool. Until more accurate methods are available, careful application and interpretation of the results of these codes are needed.

REFERENCES

1. Henderson, W. P.; and Patterson, J. C., Jr.: Propulsion Installation Characteristics for Turbofan Transports. AIAA Paper No. 83-0087, 1983.

2. Flechner, S. G.; Patterson, J. C., Jr.; and Fouinier, P. G.: NASA Conference Publication 2172, October 1980, pp. 105-121.

3. Jameson, A.; Schmidt, W.; and Turkel, E.: Numerical Solutions of the Euler Equations by Finite Volume Methods using Runge-Kutta Time-Stepping Schemes. AIAA Paper No. 81-1259, 1981.

4. Yu, N. J.; Samant, S. S.; and Rubbert, P. E.: Flow Prediction for Propfan Configurations using Euler Equations. AIAA Paper No. 84-1645, 1984.

5. Jameson, A.; and Caughey, D. A.: A Finite Volume Method for Transonic Potential Flow Calculations. AIAA Paper No. 77-635, July 1977.

6. Green, J. E.; Week, D. J.; and Brooman, J. W. F.: Prediction of Turbulent Boundary Layers and Wakes in Compressible Flow by a Lag-Entrainment Method. A.R.C.R. and M. 3791, 1977.

7. Maskew, B.: A Three-Dimensional Viscous/Potential Flow Interaction Analysis Method for Multi-Element Wings; Modification to the Potential Flow Code to Allow Part-Span, High-Lift Devices and Close-Interference Calculations. NASA CR-152277, March 1979.

8. Maskew, B.: Prediction of Subsonic Aerodynamic Characteristics: A Case for Low-Order Panel Methods. J. Aircr., vol. 19, no. 2, February 1982, pp. 157-163.

9. Cumpsty, N. A.; and Head, M. R.: The Calculation of Three-Dimensional Turbulent Boundary Layers, Part I: Flow over the Rear of an Infinite Swept Wing. Aero. Quarterly, vol. XVIII, February 1967.

10. Boppe, C. W.: Transonic Flow Field Analysis for Wing-Fuselage Configurations. NASA CR-3243, May 1980.

11. Bradshaw, P.; and Ferriss, D. H.: Calculation of Boundary Layer Development Using the Turbulent Energy Equation Compressible Flow on Adiabatic Walls. J. Fld. Mech., vol. 46, 1971.

12. Nash, J. F.; and Tseng, R. R.: The Three-Dimensional Turbulent Boundary Layer on an Infinite Yawed Wing. Aero. Quarterly, November 1971, pp. 346-362.

13. Waggoner, E. G.: Validation of a Transonic Analysis Code for use in Preliminary Design of Advanced Transport Configurations. Paper presented at the 14th ICASE Congress, Toulouse, France; September 1984.

14. Waggoner, E. G.: Computational Transonic Analysis for a Supercritical Transport Wing-Body Configuration. AIAA Paper No. 80-0129, 1980.

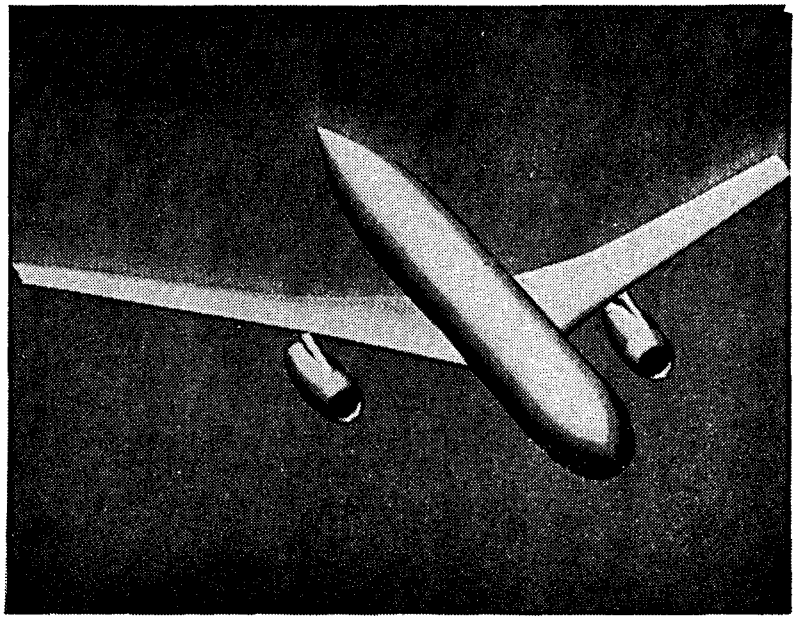

Figure 1.- Energy efficient transport (EET).

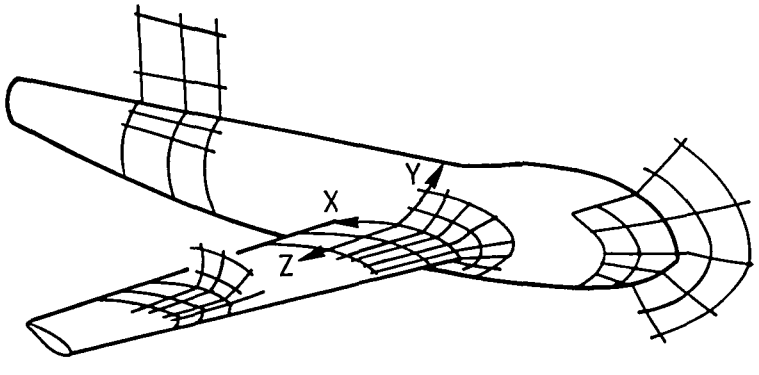

Figure 2.- Surface grid structure for Euler code.

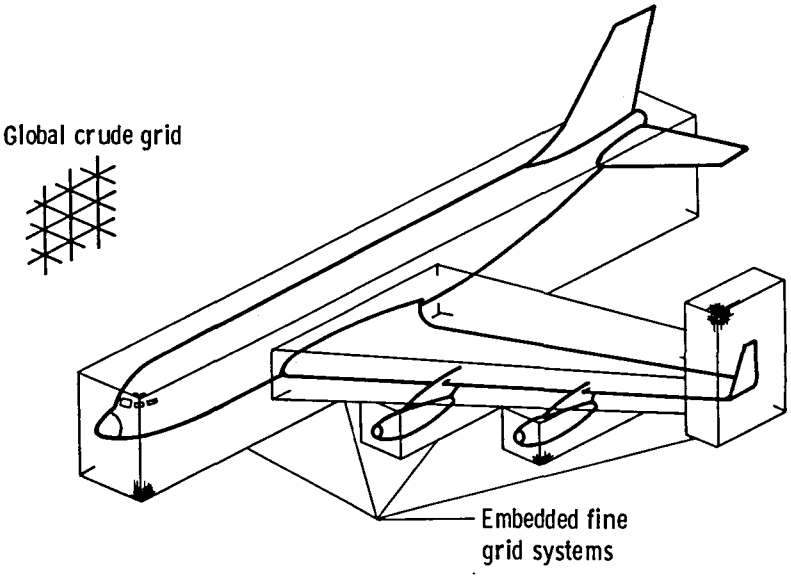

Figure 3.- Grid systems for PPW code.

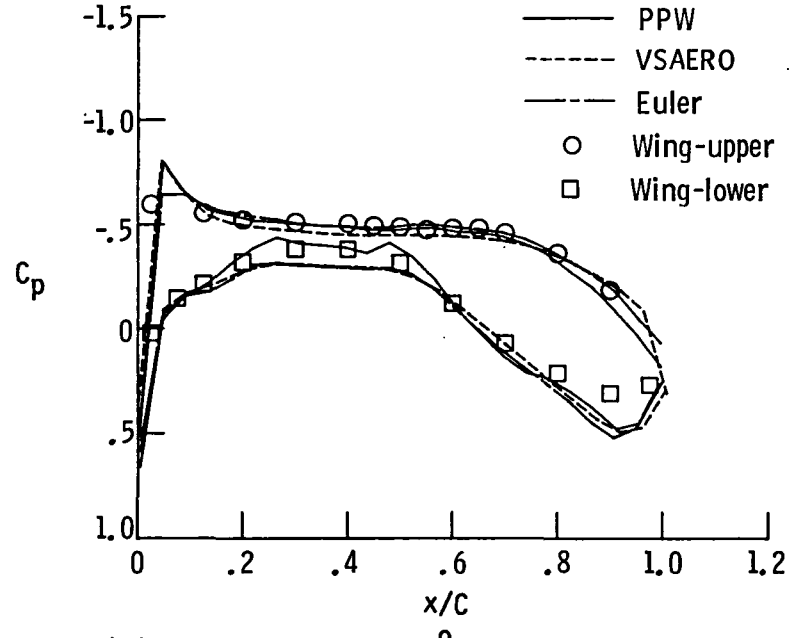

(a) $M_\infty = 0.70$, $\alpha = 1^0$, WB, Viscous.

Figure 4.- Effect of configuration and flight condition.

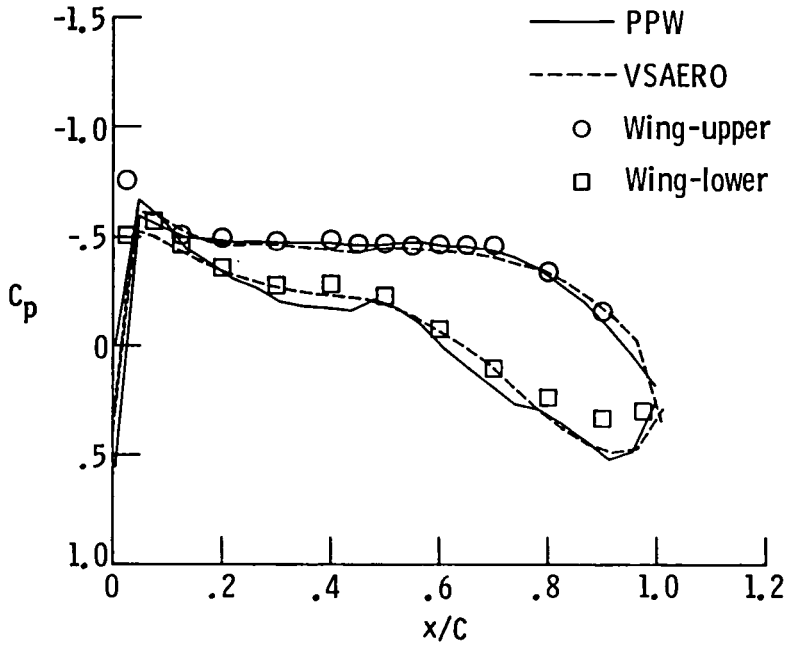

(b) $M_\infty = 0.70$, $\alpha = 1^o$, WBPN, Viscous.

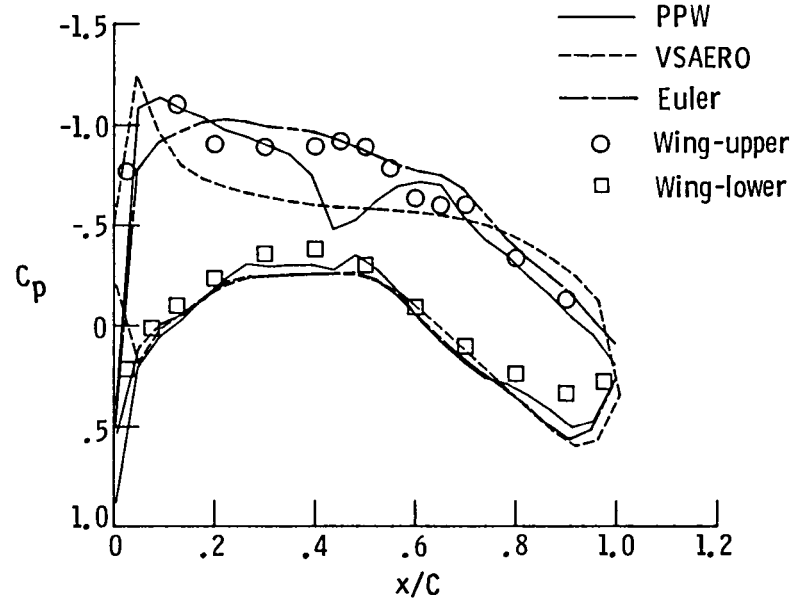

(c) $M_\infty = 0.82$, $\alpha = 2.8^o$, WB, Viscous.

Figure 4.- Continued.

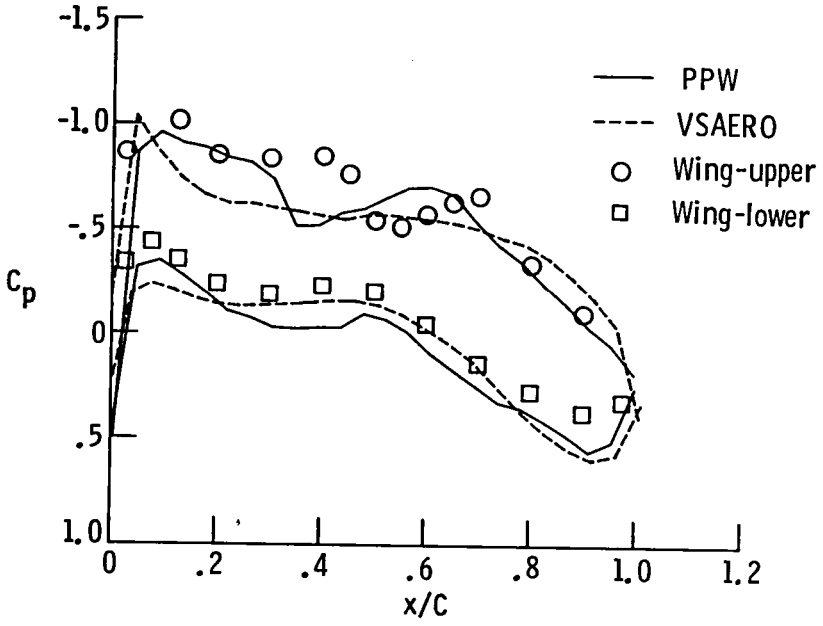

(d) $M_\infty = 0.82$, $\alpha = 2.8^o$, WBPN, Viscous.

Figure 4.- Concluded.

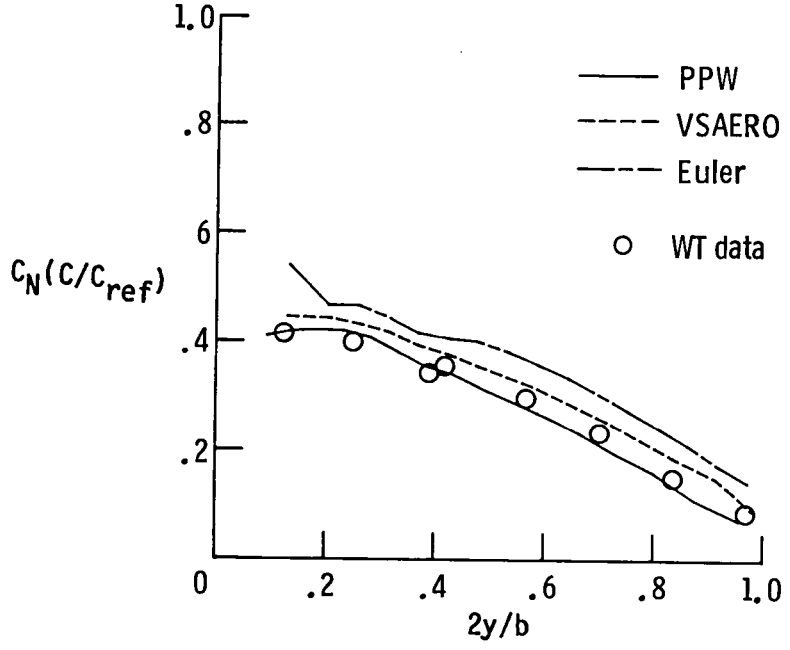

(a) $M_\infty = 0.70$, $\alpha = 1^o$, WB, Viscous.

Figure 5.- Effect of configuration and flight condition on span loading.

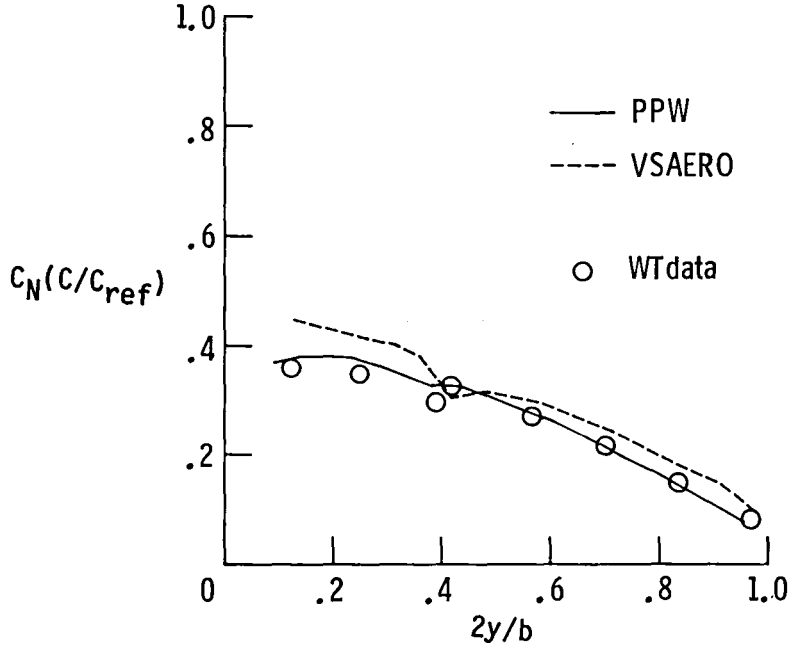

(b) $M_\infty = 0.70$, $\alpha = 1^0$, WBPN, Viscous.

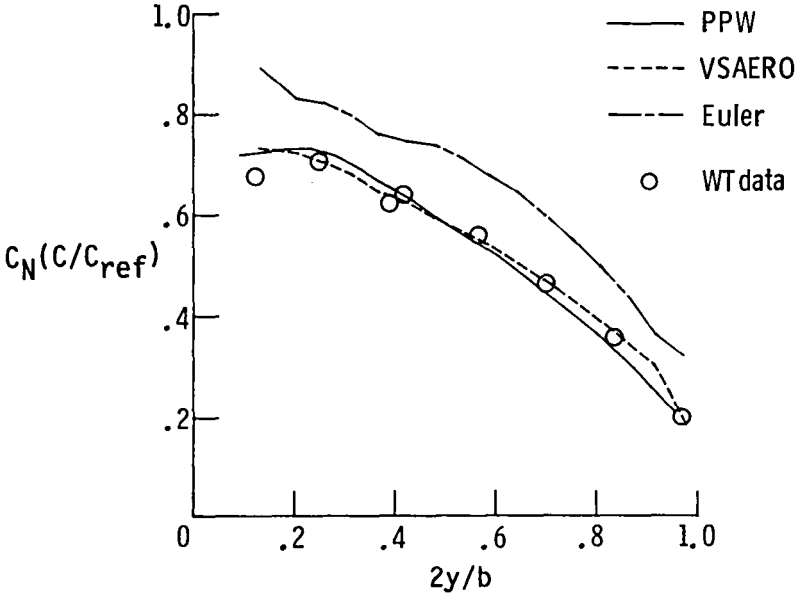

(c) $M_\infty = 0.82$, $\alpha = 2.8^0$, WB, Viscous.

Figure 5.- Continued.

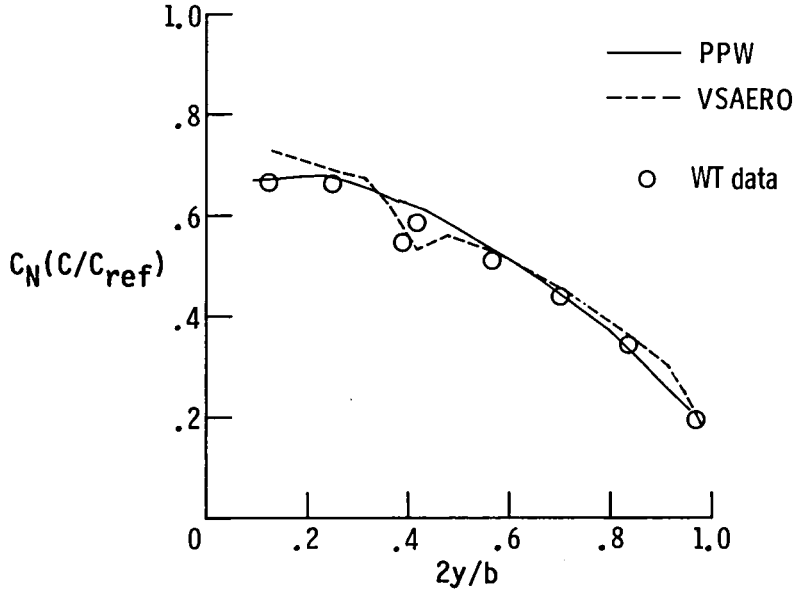

(d) $M_\infty = 0.82$, $\alpha = 2.8^o$, WBPN, Viscous.

Figure 5.- Concluded.

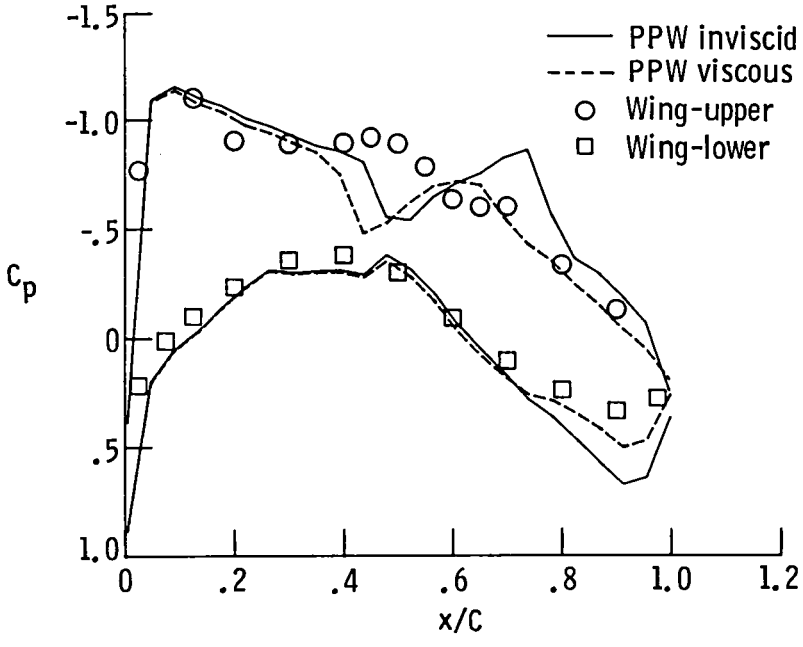

(a) $M_\infty = 0.82$, $\alpha = 2.8^o$, WB, PPW.

Figure 6.- Effect of viscosity.

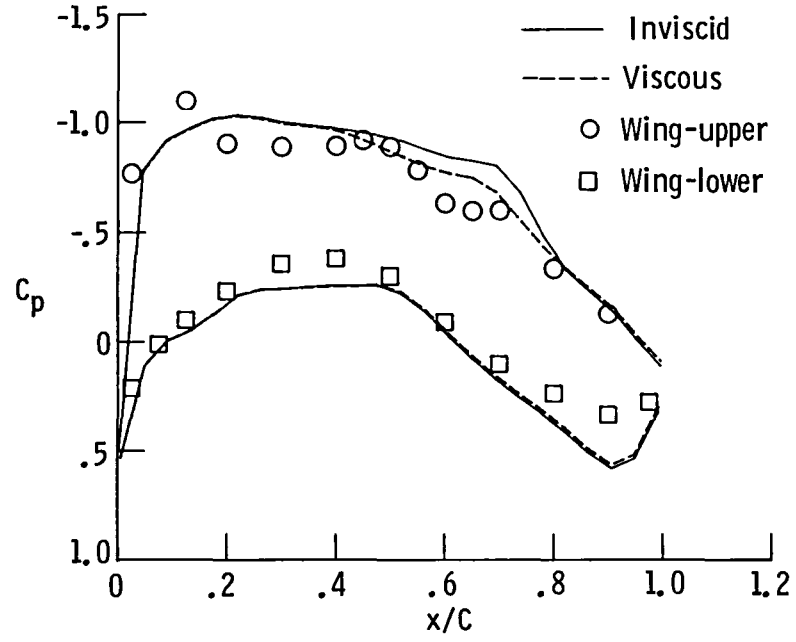

(b) $M_\infty = 0.82$, $\alpha = 2.8^o$, WB, Euler.

Figure 6.- Concluded.

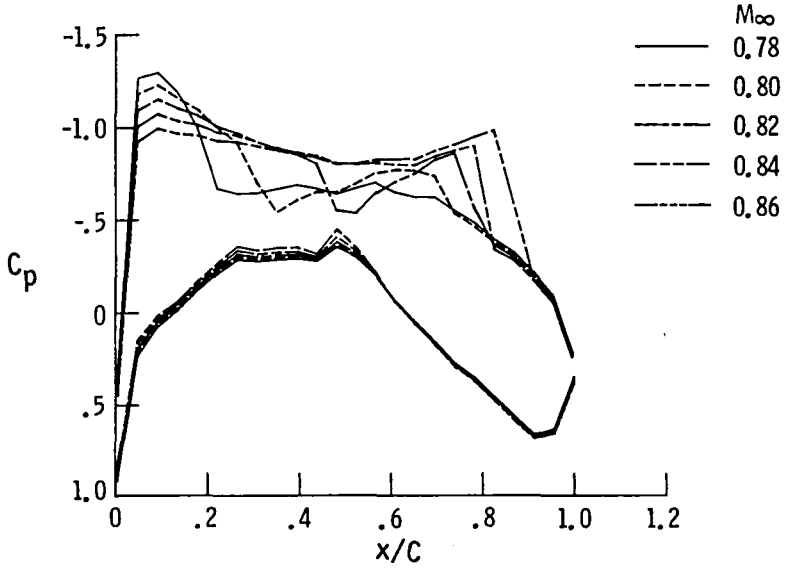

(a) $\alpha = 2.8^o$, WB, PPW, Inviscid.

Figure 7.- Effect of Mach number.

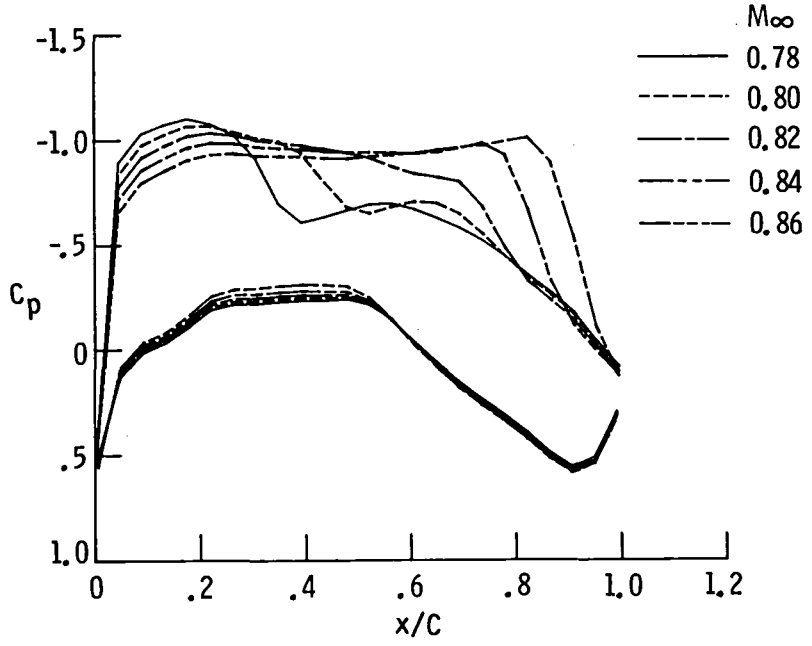

(b) $\alpha = 2.8^{o}$, Euler, WB, Inviscid.

Figure 7.- Concluded.

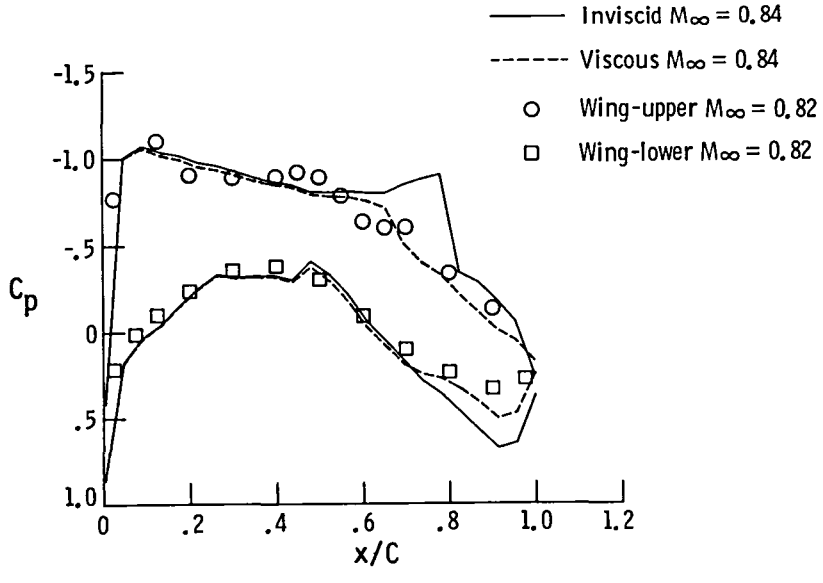

Figure 8.- Effect of viscosity at higher Mach number.
$M_{\infty} = 0.84$, $\alpha = 2.8^{o}$, PPW, WB.

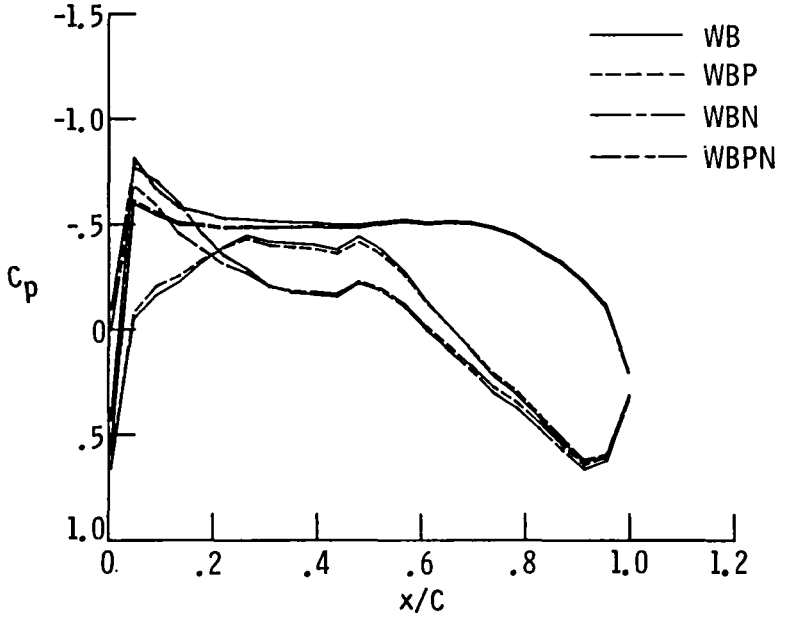

(a) $M_\infty = 0.70$, $\alpha = 1^o$, PPW, Inviscid.

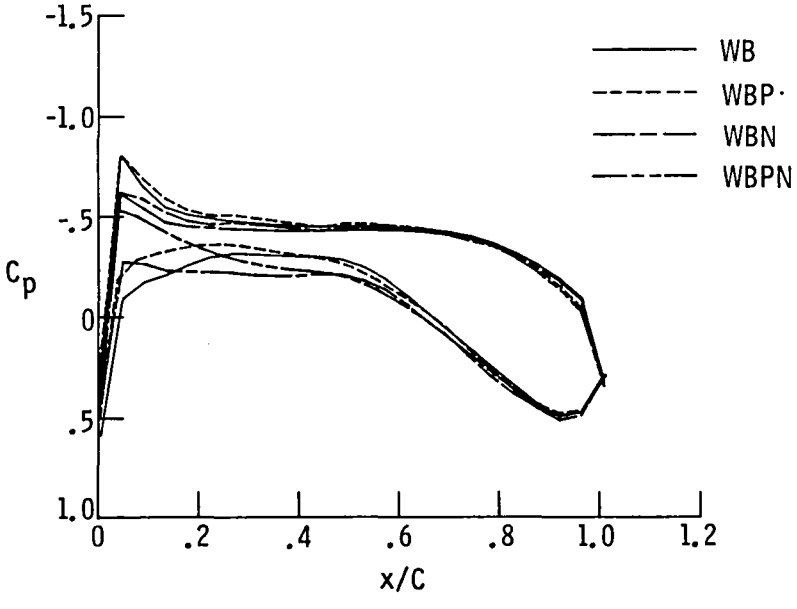

(b) $M_\infty = 0.70$, $\alpha = 1^o$, VSAERO, viscous.

Figure 9.- Effect of pylon and nacelle buildup.

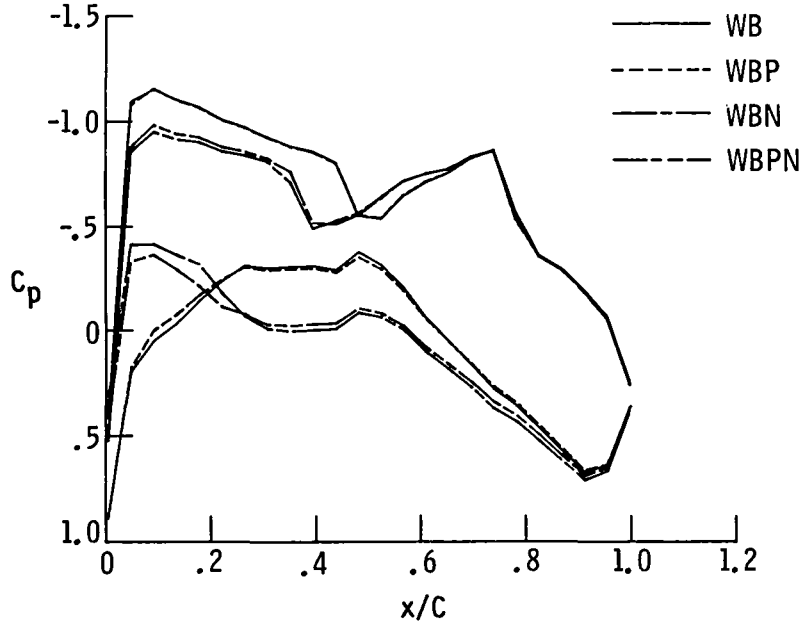

(c) $M_\infty = 0.82$, $\alpha = 2.8^o$, PPW, Inviscid.

Figure 9.- Concluded.

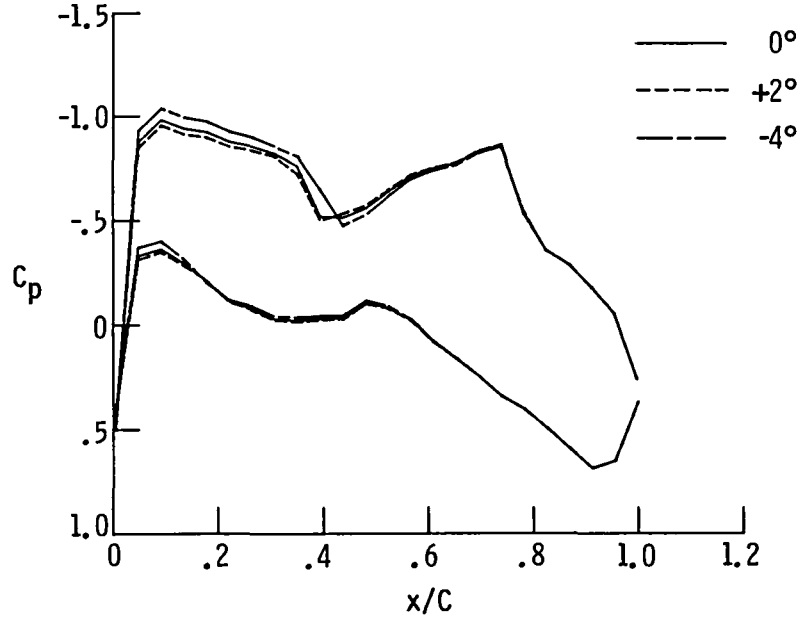

Figure 10.- Effect of nacelle incidence.
$M_\infty = 0.82$, $\alpha = 2.8^o$, PPW, Inviscid.

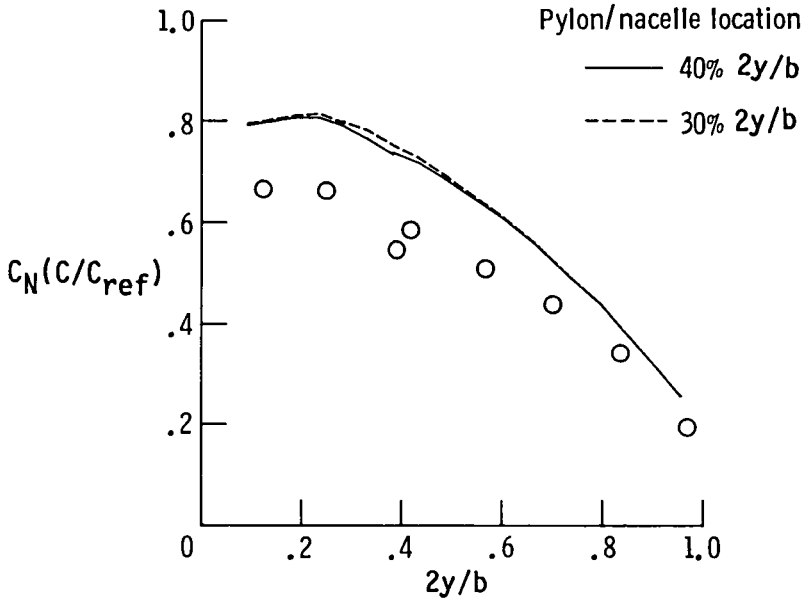

Figure 11.- Effect of Pylon/Nacelle location.

Standard Bibliographic Page

1. Report No.	2. Government Accession No.	3. Recipient's Catalog No.
NASA TM-87727		

4. Title and Subtitle	5. Report Date
EVALUATION OF THREE NUMERICAL METHODS FOR PROPULSION INTEGRATION STUDIES ON TRANSONIC TRANSPORT CONFIGURATIONS	June 1986
	6. Performing Organization Code: 505-62-91-01
7. Author(s): Steven F. Yaros, John R. Carlson, and Balasubramanyan Chandrasekaran	8. Performing Organization Report No.
9. Performing Organization Name and Address: NASA Langley Research Center, Hampton, VA 23665	10. Work Unit No.
	11. Contract or Grant No.
12. Sponsoring Agency Name and Address: National Aeronautics and Space Administration, Washington, DC 20546	13. Type of Report and Period Covered: Technical Memorandum
	14. Sponsoring Agency Code

15. Supplementary Notes

This paper will be presented at the AIAA 4th Applied Aerodynamics Conference, June 9-11, 1986, in San Diego, California. AIAA Paper No. 86-1814.
Steven F. Yaros and John R. Carlson, NASA Langley Research Center, Hampton, VA.
Balasubramanyan Chandrasekaran, Vigyan Research Associates, Inc., Hampton, VA.

16. Abstract

An effort has been undertaken at the NASA Langley Research Center to assess the capabilities of available computational methods for use in propulsion integration design studies of transonic transport aircraft, particularly of pylon/nacelle combinations which exhibit essentially no interference drag. The three computer codes selected represent state-of-the-art computational methods for analyzing complex configurations at subsonic and transonic flight conditions. These are: EULER, a finite volume solution of the Euler equation; VSAERO, a panel solution of the Laplace equation; and PPW, a finite difference solution of the small disturbance transonic equations. In general, all three codes have certain capabilities that allow them to be of some value in predicting the flows about transport configurations, but all have limitations. Until more accurate methods are available, careful application and interpretation of the results of these codes are needed.

17. Key Words (Suggested by Authors(s))	18. Distribution Statement
Applied aerodynamics Propulsion integration Numerical methods	Unclassified - Unlimited Subject Category 02

19. Security Classif.(of this report)	20. Security Classif.(of this page)	21. No. of Pages	22. Price
Unclassified	Unclassified	22	A02

For sale by the National Technical Information Service, Springfield, Virginia 22161

End of Document